Research Paper

Journal of Vascular Research

J Vasc Res
DOI: 10.1159/000353295

Received: January 21, 2013
Accepted after revision: April 30, 2013
Published online: ■■■

Long-Term Remodeling of Rat Pial Microcirculation after Transient Middle Cerebral Artery Occlusion and Reperfusion

D. Lapi[a] S. Vagnani[c] D. Sapio[a] T. Mastantuono[a] L. Sabatino[b] M. Paterni[d] A. Colantuoni[a]

[a]Department of Neuroscience, 'Federico II' University Medical School, Naples, [b]Department of Biochemistry, Sannio University, Benevento, [c]Department of Internal Medicine, Rheumatology Unit, University of Pisa, and [d]CNR Institute of Clinical Physiology, Pisa, Italy

Key Words
Microcirculation · Brain · Ischemia-reperfusion · Remodeling · Nitric oxide synthase

Abstract
Objective: The aim of this study was to assess the in vivo structural and functional remodeling of pial arteriolar networks in the ischemic area of rats submitted to transient middle cerebral artery occlusion (MCAO) and different time intervals of reperfusion. ***Methods and Results:*** Two closed cranial windows were implanted above the left and right parietal cortex to observe pial microcirculation by fluorescence microscopy. The geometric characteristics of pial arteriolar networks, permeability increase, leukocyte adhesion and capillary density were analyzed after 1 h or 1, 7, 14 or 28 days of reperfusion. MCAO and 1-hour reperfusion caused marked microvascular changes in pial networks. The necrotic core was devoid of vessels, while the penumbra area presented a few arterioles, capillaries and venules with severe neuronal damage. Penumbra microvascular permeability and leukocyte adhesion were pronounced. At 7 days of reperfusion, new pial arterioles were organized in anastomotic vessels, overlapping the ischemic core and in penetrating pial arterioles. Vascular remodeling caused different arteriolar rearrangement up to 28 days of reperfusion and animals gradually regained their motor and sensory functions. ***Conclusions:*** Transient MCAO-induced pial-network remodeling is characterized by arteriolar anastomotic arcades. Remodeling mechanisms appear to be accompanied by an increased expression of nitric oxide synthases.

Introduction

Cerebral stroke has been studied in several experimental models, where particular attention has been devoted to neuronal dysfunctions, metabolic events and vascular involvement [1–3]. Edema formation, cellular swelling and microvascular damage have been extensively evaluated [4, 5]. Most studies, however, have been focused on neuronal damage, while no angiogenesis has been documented for areas near the ischemic core, such as the necrotic area induced by middle cerebral artery occlusion (MCAO) [6]. The growth of new blood vessels after a stroke could be interpreted as a natural defense mechanism helping to restore the oxygen and nutrient supply to the affected brain tissue [7]. Some studies using either mice or rats with transient or permanent MCAO demon-

KARGER

E-Mail karger@karger.com
www.karger.com/jvr

1018–1172/13/0000–0000$38.00/0

Dr. Dominga Lapi
Department of Neuroscience, 'Federico II' University Medical School
Via S. Pansini, 5
IT–80131 Naples (Italy)
E-Mail d.lapi@dfb.unipi.it

strated that endothelial cells surrounding the infarcted brain area start to proliferate as early as 12–24 h following vessel damage [8, 9]. This, in turn, already leads to an increase of vessels in the peri-infarcted region at 3 days following the ischemic injury. Studies using human brain samples have demonstrated that active angiogenesis takes place 3–4 days after the ischemic insult [10]. It is not clear how long-lasting angiogenesis actively occurs in the injured brain because long-term studies have not been performed. Hayashi et al. [8] described that vessel proliferation continued for more than 21 days following experimental cerebral ischemia.

Previously, Tomita et al. [11], utilizing a confocal microscope to observe the mouse cerebral circulation through a closed cranial window chronically implanted over the left parieto-occipital cortex, demonstrated that vascular remodeling of microvessel networks in the ischemic area is visible on day 30 after permanent MCAO.

Conversely, further methods of analysis, such as cDNA arrays, RT-PCR, Western blot and immunohistochemistry suggested that nitric oxide (NO) is involved in ischemic brain damage and can exert both protective and deleterious effects depending on factors such as the NO synthase (NOS) isoforms and the cell type where NO is produced or the temporal stage after the onset of the ischemic brain injury. Immediately after brain ischemia, NO release from endothelial NOS (eNOS) is protective mainly due to promoting vasodilation; however, after ischemia develops, NO produced by the overactivation of neuronal NOS (nNOS) and NO release by the de novo expression of inducible NOS (iNOS) later contribute to the brain damage [12–15]. An increase in vascular endothelial growth factor (VEGF) expression has been observed in both animal and human models – representing one of the most important factors in the process of angiogenesis – in the infarcted hemisphere as early as 3 h after an ischemic insult and continuing for up to 3 or 7 days [9, 16, 17]. Moreover, the VEGF expression appears to trigger an NO-dependent mechanism [18]. Therefore, eNOS and VEGF are involved in the cerebral vascular remodeling after ischemia, but the spatial and temporal dynamics of poststroke cerebral microvascular rearrangement and the molecular factors involved are complex and remain incompletely characterized.

This study was carried out to evaluate the in vivo structural and functional reorganization of pial arteriolar networks in the ischemic area of rats subjected to MCAO, assessed at different time intervals during reperfusion. Geometric remodeling of pial arterioles were evaluated as well as microvascular permeability, leukocyte adhesion to venular walls and perfused capillary density (PCD), the main indexes of cerebral microcirculation damage resulting in perivascular edema, vessel wall failure and reduction in tissue perfusion, respectively [19, 20]. Furthermore, pial arteriolar functions were assessed testing endothelial and smooth muscle cell response to topical acetylcholine (Ach) or papaverine (Pap). We correlated these vascular observations with the determination of VEGF, eNOS, nNOS and iNOS expression to clarify their role during pial arteriolar network reorganization [21].

According to previous suggestions, angiogenic vessels provide neurotrophic support to pre-existent or newly generated neurons, while neuroblasts have been found to be concentrated around the blood vessels following a stroke [7, 22]. Therefore, to estimate the brain functions accompanied by pial microvascular network remodeling, we calculated the modified neurological severity scores [23].

Materials and Methods

Experimental Groups

Six groups of rats were studied. The first group, sham-operated animals (S group, n = 26), underwent the same procedures as the other experimental groups without MCAO. The following groups of animals were subjected to 2 h of MCAO and 1 h (R1h group, n = 26), 1 day (R1day group, n = 26), 7 days (R7day group, n = 26), 14 days (R14day group, n = 26) or 28 days (R28day group, n = 26) of reperfusion.

In each experimental group, 7 animals were utilized for microvascular studies, 6 rats to test the pial arteriolar responses to topically applied Ach (10^{-6} M, n = 3) or Pap (10^{-4} M, n = 3) [24, 25]. Finally, 10 animals belonging to each experimental group were used to evaluate VEGF (n = 5), eNOS (total and phosphorylated) (n = 10), nNOS (n = 10) and iNOS (n = 10) expression by Western blotting and 3 animals were used to determine neuronal damage by 2,3,5-triphenyltetrazolium chloride (TTC) staining.

Animal Preparation

Anesthesia was induced in male Wistar rats [250- to 300-gram body weight (b.w.)] with intraperitoneal (i.p.) alpha-chloralose (60 mg/kg b.w.). MCAO was induced by the intraluminal filament method as described by Longa et al. [26] and Garcia et al. [27]. Briefly, a 4–0 monofilament nylon thread with a rounded tip was inserted into the external carotid artery and gently advanced about 20 mm to interrupt the blood flow of the left middle cerebral artery. After 2 h of occlusion, the filament was pulled out to allow reperfusion.

To determine the perfusion decrease during MCAO, microvascular blood flow was measured by laser Doppler perfusion monitoring on the skull of all animals by a Perimed PF5001 flowmeter, using a probe (407; Perimed, Sweden) attached to the bone. The sampling rate was 32 Hz and blood flow was expressed as perfusion units. Applying the probe on the ischemic hemisphere of the skull, it was possible to identify and quantify blood flow within the ischemic core where the amount of residual blood flow during occlu-

sion was typically in a range of 15–20% of the baseline. In all experimental groups, we determined the blood flow in the ischemic core. The penumbra blood flow is usually higher than 25–35% of the baseline, as previously reported [28]. After 2 h of ischemia, the intraluminal filament was withdrawn and the incision sutured, except in the animals studied immediately after MCAO. Successively, the rats were allowed to recover from surgical intervention with free access to pellets and water. After 1, 7, 14 or 28 days of reperfusion, the animals were again anesthetized (alpha-chloralose 60 mg/kg b.w., i.p.) for pial microcirculation observation.

All experiments were conducted according to the Guide for the Care and Use of Laboratory Animals published by the US National Institutes of Health (NIH Publication No. 85-23, revised 1996) and the institutional rules for the care and handling of experimental animals. The protocol was approved by the 'Federico II' University of Naples ethical committee.

Closed Cranial-Window Preparation

Under anesthesia, the animals were tracheotomized, intubated and mechanically ventilated with room air and supplemental oxygen.

A catheter was placed in the left femoral artery for recording arterial blood pressure and sampling of blood gases, another was placed in the right femoral vein for injection of the fluorescent tracers [fluorescein isothiocyanate bound to dextran, molecular weight 70 KDa (FD 70), 50 mg/100 g b.w. i.v. as a 5% weight/volume solution in 5 min and rhodamine 6G to label leukocytes 1 mg/100 g b.w. in 0.3 ml] and for additional anesthesia. Blood gas measurements were carried out on arterial blood samples withdrawn from the arterial catheter at time intervals of 30 min (ABL5; Radiometer, Copenhagen, Denmark). Mean arterial blood pressure (MABP), heart rate, respiratory CO_2 and blood gas values were recorded and were kept stable within physiological ranges. Rectal temperature was monitored and preserved at 37.0 ± 0.5°C with a heating stereotaxic frame, to which the rats were secured.

To observe pial microcirculation, a closed cranial window (4 × 5 mm) was implanted above the left parietal cortex (posterior 1.5 mm to bregma and lateral 3 mm to the midline) [29]. Successively, a second closed cranial window was fixed, obeying the same spatial coordinates as the previous one, above the right parietal cortex to visualize the contralateral pial microcirculation. The dura mater was gently removed and a 150-μm-thick quartz microscope coverglass was sealed to the bone with dental cement. The window inflow and outflow were assured by two needles secured in the dental cement of the window so that the brain parenchyma was continuously superfused with artificial cerebrospinal fluid (aCSF). The rate of superfusion was 0.5 ml/min controlled by a peristaltic pump. During superfusion, the intracranial pressure was maintained at 5 ± 1 mm Hg and measured by a pressure transducer connected to a computer. The composition of the aCSF was: 119.0 mM NaCl, 2.5 mM KCl, 1.3 mM $MgSO_4 \cdot 7H_2O$, 1.0 mM NaH_2PO_4, 26.2 mM $NaHCO_3$, 2.5 mM $CaCl_2$ and 11.0 mM glucose (equilibrated with 10% O_2, 6% CO_2 and 84% N_2; pH 7.38 ± 0.02). The temperature was maintained at 37.0 ± 0.5°C [30].

Fluorescence Microscopy and Microvascular Parameter Assessment

Pial microcirculation was visualized with a fluorescence microscope (Leitz Orthoplan) fitted with long-distance objectives [×2.5, numerical aperture (NA) 0.08; ×10, NA 0.20; ×20, NA 0.25; ×32, NA 0.40], a ×10 eyepiece and a filter block (Ploemopak, Leitz). Epi-illumination was provided by a 100-watt mercury lamp using the appropriate filters for FITC, for rhodamine 6G and a heat filter (Leitz KG1). Pial microcirculation was televised with a DAGE MTI 300RC low-light-level digital camera and recorded by a computer-based frame-grabber (Pinnacle DC 10 Plus, Avid Technology, Mass., USA).

Video images were videotaped and microvascular measurements (diameter and length) were made off-line using a computer-assisted imaging software system (MIP Image, CNR, Institute of Clinical Physiology, Pisa, Italy). The results of diameter measurements agreed with those obtained by the shearing method (± 0.5 μm).

The arteriolar network was mapped by stop-frame images and pial arterioles were classified according to a centripetal ordering scheme (Strahler method, modified according to diameter) [31]. Order 0 was assigned to the capillaries; thereafter, the terminal arterioles were assigned order 1 and the vessels upstream were each assigned a progressively higher order. When two vessels of the same order joined, the parent vessel was assigned the next higher orders. If two daughter vessels were of different orders, the parent vessel retained the higher of the two. The procedure of the pial arteriole classification has been reported previously [32]. A 'connectivity matrix' was also calculated to clarify the number and order of daughter arterioles spreading from parent vessels. Briefly, order n vessels may spring from orders $n + 1$, $n + 2$, … vessels, the component of which in row n and column m was the ratio of the total number of elements of order n sprung from elements in order m [32] (see Appendix for more details).

Penetrating pial arterioles, i.e. pial arterioles supplying the outer layers of the cerebral cortex, were enumerated under baseline conditions and at the different times of reperfusion by a computer-assisted method. The analysis was carried out counting the pial arterioles penetrating into the cortex subsurface in a region of interest (ROI) of 400 μm^2 [33].

The increase in permeability was calculated and reported as normalized grey levels (NGL): NGL = (I–Ir)/Ir, where Ir is the average baseline grey level at the end of vessel filling with fluorescence (average of 5 windows located outside the blood vessels with the same windows being used throughout the experimental procedure), and I is the same parameter at the end of reperfusion. Grey levels ranging from 0 to 255 were determined by the MIP Image program in five ROIs measuring 50 μm^2 (×10 objective). The same location of ROI during recordings along the microvascular networks was provided by a computer-assisted device for XY movement of the microscope table.

Adherent leukocytes (i.e. cells on vessel walls that did not move over a 30-second observation period) were quantified in terms of number/100 μm of venular length (v.l.)/30 s using a higher magnification (×32, microscope objective). In each experimental group, 45 venules were studied. The PCD was measured by a computerized method (MIP Image) in an area of 150 cm^2 and expressed as $cm/cm^2 = cm^{-1}$.

The single pial venule blood flow (SBF), Q, was calculated according to the following equation: $Q = \alpha \times V_{CL} \times A$, where α was a constant, related to the vessel diameter, V_{CL} was the red blood cell centerline velocity and A was the cross-sectional area. SBF was calculated in the venules with a diameter of 30–40 μm in both the left and right hemispheres. In rats subjected to MCAO and reperfusion, SBF in the affected hemisphere was compared to that in the contra-

lateral hemisphere. Previous data indicate that SBF may be an accurate measure of pial blood flow drainage from the cerebral cortex, because it represents about 30–60% of the cortical blood flow. Therefore, we chose to measure the SBF to compare with laser Doppler perfusion monitoring data and to estimate the difference in blood flow between the affected and the nonaffected hemisphere.

Finally, pial arteriolar reactivity was tested by topically applied Ach (10^{-6} M, n = 3) or Pap (10^{-4} M, n = 3). To avoid a bias due to single-operator measurements, two independent 'blinded' operators measured all the microvascular parameters. Their measurements overlapped in all cases.

MABP (Viggo-Spectramed P10E2 transducer, Oxnard, Calif., USA; connected to a catheter in the femoral artery) and heart rate were monitored with a Gould Windograf recorder (model 13-6615-10S, Gould, Ohio, USA). Data were recorded and stored in a computer. Blood gas measurements (arterial partial pressure of O_2 and CO_2 and pH) were carried out on arterial blood samples withdrawn from the arterial catheter at 30-min intervals (ABL5, Radiometer, Copenhagen, Denmark).

Western Blot Analysis

Expression of all investigated proteins was monitored at the indicated time points by Western blot. Proteins were extracted from brain tissue with lysis buffer and then incubated for 30 min on ice [34]. The supernatant was isolated by centrifugation at 13,000 *g* for 10 min at 4°C. The concentration of total protein in each sample was quantified by the Lowry method. Equal amounts of proteins were separated by SDS-PAGE under reducing conditions, and then transferred to polyvinylidene difluoride membranes (PVDF, Invitrogen). The membrane was blocked for 1 h in 5% non-fat milk in Tris-buffered saline and 0.1% Tween 20 (TBST) at 4°C. Filters were incubated with specific antibodies at 4°C overnight, before being washed 3 times in TBST and then incubated with horseradish peroxidase-conjugated secondary antibody (1:2,000) (GE-Healthcare, Little Chalfont, UK) for 1 h at room temperature. After triple washing with TBST, peroxidase activity was detected with the ECL system (GE-Healthcare). The optical density of the bands was determined by the ChemiDoc Imaging System (Bio-Rad). By incubating PVDF membrane in parallel with the extracellular signal-regulated kinase (ERK) antibody (1:5,000), normalization of results was obtained. Specific antibodies were: mouse monoclonal anti-VEGF (1:200), rabbit polyclonal anti-eNOS (1:500), rabbit polyclonal anti-phosphorylated eNOS (Ser 1177) (1:250), mouse monoclonal anti nNOS (1:1,000) and rabbit polyclonal anti iNOS (1:500). Antibodies were purchased from Santa Cruz Biotechnology, Santa Cruz, Calif., USA.

TTC Staining

Rats were sacrificed after 2-hour MCAO and at different times during reperfusion. Tissue damage was evaluated by TTC staining. The brains were cut into 1-mm coronal slices with a vibratome (Campden Instrument, 752 M). Sections were incubated in 2% TTC for 20 min at 37°C and in 10% formalin overnight. The necrotic area site and extent in each section were evaluated by image analysis software (Image-Pro Plus) [35]. Infarct size was quantified by manual measurement as previously reported [35] and expressed as a percentage according to the following formula: (area of the ischemic lesion:area of hemisphere ipsilateral to the lesion = X:100).

Table 1. Diameter, length and branching ratios in the different experimental groups

Group	Ratio		
	diameter	length	branching
S	1.39	1.70	1.62
R1h	undetectable	undetectable	undetectable
R1day	1.36*	1.68*	1.58*
R7day	1.37*	2.04*	1.60*
R14day	1.37*	2.03*	1.61
R28day	1.39	2.02*	1.60*

* $p < 0.01$ vs. S group.

Neurological Assessment

All animals were subjected to a battery of behavioral tests before MCAO and at different reperfusion times, using a modified neurological severity score, as previously described by Chen et al. [23]. Briefly, this score is derived by evaluating animals for hemiparesis (the response to raising the rat by the tail or placing the rat on a flat surface), sensory deficits (placing and proprioception), beam balance test (the response to placement and posture on a narrow beam and the time before falling off it), absent reflexes (pinna, corneal and startle) and abnormal movement (seizure, myoclonus and myodystony). One point is awarded for the inability to perform a task or for the lack of a tested reflex.

Statistical Analysis

All data were expressed as mean ± SEM. Data were tested for normal distribution with the Kolmogorov-Smirnov test. Parametric (Student t tests, ANOVA and Bonferroni post hoc test) or nonparametric tests (Wilcoxon, Mann-Whitney and Kruskal-Wallis tests) were used; nonparametric tests were applied to compare diameter and length data among experimental groups. The statistical analysis was carried out by SPSS 14.0 statistical package. Statistical significance was set at $p < 0.05$.

Results

The S Group

In the S group, pial arteriolar networks showed the same geometric characteristics when observed on left or right parietal hemisphere. Pial arterioles, seldom organized in arcading vessels (especially order 2 and order 1 arterioles), were classified according to diameter, length and branching. Order 0 was assigned to the capillaries; subsequently, the terminal arterioles were assigned order 1 (mean diameter: 15.5 ± 0.7 μm) and the vessels upstream were assigned progressively higher orders (mean diameter: 23.0 ± 0.5, 34.0 ± 0.6 and 44.5 ± 0.7 μm for orders 2, 3 and 4, respectively) (table 1).

Table 2. Connectivity matrix with 4 orders of pial arterioles in the affected hemisphere

Order *n*	Order *m*			
	1	2	3	4
a S group				
0	2.28±0.40 (89)	0.23±0.15 (7)	0	0
1	0.21±0.11 (8)	2.06±0.54 (64)	0.65±0.18 (17)	0.49±0.11 (5)
2	0	0.25±0.10 (8)	1.79±1.00 (46)	1.43±0.70 (14)
3	0	0	0.40±0.16 (10)	2.50±0.90 (25)
4	0	0	0	0.15±0.08 (1)
Order 1: 39 vessels; order 2: 31 vessels; order 3: 26 vessels; order 4: 10 vessels.				
b R1day group				
0	1.81±0.62 (38)	0.13±0.08 (2)	0	0
1	0.18±0.07 (4)	1.50±0.60 (24)	1.15±0.40 (22)	0.11±0.06 (1)
2	0	0	1.00±0.56 (19)	1.90±0.38 (13)
3	0	0	0	1.20±0.43 (8)
4	0	0	0	0.10±0.05 (1)
Order 1: 21 vessels; order 2: 16 vessels; order 3: 19 vessels; order 4: 7 vessels.				
c R7day group				
0	1.94±0.30 (45)	0.70±0.09 (13)	0	0
1	0.38±0.14 (9)	0.89±0.13 (16)	1.27±0.25 (25)	0.31±0.11 (2)
2	0	0.62±0.17 (11)	0.25±0.12 (5)	1.55±0.42 (11)
3	0	0	0.36±0.13 (7)	0.20±0.08 (1)
4	0	0	0	0
Order 1: 23 vessels; order 2: 18 vessels; order 3: 20 vessels; order 4: 7 vessels.				
d R14day group				
0	2.43±0.32 (73)	1.12±0.11 (21)	0	0
1	0.45±0.12 (13)	0.94±0.29 (18)	1.86±0.13 (41)	0.48±0.20 (4)
2	0	0.35±0.15 (7)	0.54±0.12 (12)	1.77±0.21 (16)
3	0	0	0.60±0.22 (13)	1.57±0.40 (14)
4	0	0	0	0
Order 1: 30 vessels; order 2: 19 vessels; order 3: 22 vessels; order 4: 9 vessels.				
e R28day group				
0	2.22±0.38 (69)	0.25±0.12 (4)	0	0
1	0.33±0.14 (10)	0.52±0.12 (9)	0.28±0.11 (7)	0
2	0	0.28±0.15 (5)	1.24±0.80 (30)	0.66±0.23 (7)
3	0	0	0.29±0.10 (7)	1.33±0.46 (15)
4	0	0	0	0.33±0.10 (4)
Order 1: 31 vessels; order 2: 18 vessels; order 3: 24 vessels; order 4: 11 vessels.				

Values in connectivity matrix are means ± SEM. An element *(m, n)* in row *m* and column *n* is the ratio of the total number of elements of order *m* that spring directly from parent elements of order *n* divided by the total number of elements of order *n*. The total numbers of vessels of order *n* originating from parent arterioles of order *m* are reported in parentheses.

Table 3. Anastomotic and penetrating arterioles present in each experimental preparation at the different reperfusion times or originating from anastomotic order 2 and order 1 vessels

Group	Anastomotic arterioles, n		Penetrating arterioles, n		Order 2 anastomotic arterioles, n		Order 1 anastomotic arterioles, n
	order 1	order 2	order 1	order 2	order 1	order 2	order 1
S group	2.14±0.9	1.7±0.8	10±1	7±2	3.2±0.5	2.2±0.7	0.5±0.2
R1h	undetectable	undetectable	undetectable	undetectable	undetectable	undetectable	undetectable
R1day	undetectable	undetectable	3±2*	2±1*	undetectable	undetectable	undetectable
R7day	2.7±0.9	2.6±1.0	4±1*	3±1*	5.4±0.4 *	3.3±0.3	0.3±0.1
R14day	6.4±1.3*	3.8±1.1	6±1*	4±2*	8.8±0.7 *	5.1±0.5 *	7.1±0.6*
R28day	7.7±2.5*	5.1±1.0*	14±1*	12±1*	12.8±0.8 *	6.8±0.9 *	12.3±0.8*

* $p < 0.01$ vs. S group.

Table 4. Summary of the principal parameters in each experimental group

Group	Microvascular permeability (NGL)	Leukocyte adhesion, number of leukocytes/ 100 μm of venular length/30 s	PCD, cm^{-1}	Arteriolar diameter after Ach application, %	Arteriolar diameter after Pap application, %
S group	0.02±0.01	1.0±0.5	106.0±2.3	114.4±0.8	117.2±0.6
R1h	0.62±0.03*	10.0±0.5*	62.0±1.4*	undetectable	undetectable
R1day	0.50±0.03*	9.5±0.5*	61.5±1.5*	undetectable	undetectable
R7day	0.47±0.02*	8.0±0.5*	67.0± 1.0*	110.0±0.4*	113.0±0.5*
R14day	0.40±0.03*	6.0±0.5*	70.0±1.4*	111.0±0.8*	114.0±0.5*
R28day	0.20±0.02*	3.0±0.2*	85.1±1.2*	114.0±0.6	116.5±0.8

Arteriolar diameter is reported as percentage changes of 100% baseline values (baseline diameter of order 3 arterioles = 100) after topical application of Ach and Pap.

* $p < 0.01$ vs. S group.

Data obtained from the S group were pooled; the diameter (a), length (b) and branching distribution (c) in successive orders of arterioles obeyed Horton's Law, according to the following equations:

$\log_{10} D_n = a + bn$
$\log_{10} L_n = a + bn$
$\log_{10} N_n = a + bn$

where a and b are 2 constants. The logarithm of diameter, length and branching was directly proportional to the vessel order number. Diameter, length and branching ratios, calculated from the slope of curves, were 1.39, 1.70 and 1.62, respectively (table 1).

The branching vessels in the pial networks were described by connectivity matrix indicating vessel connection of one order to another; usually an order 4 arteriole gave rise to most order 3 vessels (table 2a) (an example of such a computation and all data on connectivity matrix are given in the Appendix). Moreover, each pial network showed penetrating pial arterioles, smaller vessels supplying cortex layers (table 3).

Blood brain barrier integrity was preserved in all S group animals and leukocyte adhesion was not detected (table 4). PCD was 106.1 ± 2.3 cm^{-1} (table 4). In the single pial venules (diameter 30–40 μm), the blood flow was 250.6 ± 7.5 and 249.4 ± 4.5 nl/s in left and right hemispheres, respectively (table 5).

Pial arterioles dilated after local Ach administration by 10.0 ± 0.6, 14.4 ± 0.8 and 12.0 ± 0.5% of the baseline in orders 4, 3 and 2, respectively (fig. 1a, b). Topical Pap application induced dilation by 12.0 ± 0.5, 18.0 ± 0.3 and 17.2 ± 0.6% of the baseline in orders 4, 3 and 2, respectively. All venular vessels were perfused (table 4).

MCAO and One Hour of Reperfusion

The affected hemisphere presented an ischemic core devoid of blood flow, not all core vessels were visualized

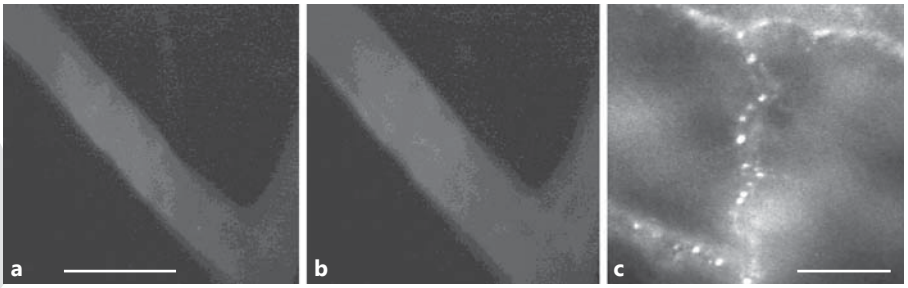

Fig. 1. Computer-assisted images of rat pial arterioles under baseline conditions (**a**) and after topical application of acetylcholine (**b**). Scale bar = 50 μm. **c** Computer-assisted image of adhered leukocytes, labeled by rhodamine 6G, to venular walls. Scale bar = 50 μm.

by fluorescent dextran; the penumbra area was characterized by a reduced blood flow (fig. 2b)

Pial microvasculature was markedly compromised; so no vessel geometric evaluation was performed and penetrating pial arterioles were not detected. Penumbra microvascular permeability was marked as well as leukocyte adhesion (table 4; fig. 1c). PCD was reduced to 62.0 ± 1.4 cm^{-1} ($p < 0.01$ vs. S group). SBF decreased by 68 ± 3% compared to the contralateral one ($p < 0.01$ vs. contralateral, 249.5 ± 8.2 nl/s) (table 5). Penumbra pial arterioles did not show any response to topically applied Ach or Pap (table 4).

Several perfused large venules were detected in the affected hemisphere penumbra when compared to the contralateral ones, where no changes in arteriolar, capillary and venular architecture and blood flow were observed.

Table 5. SBF in the affected (left) and contralateral (right) hemispheres and relative % decrease in each experimental group

Group	Left hemisphere: affected, nl/s	Right hemisphere: contralateral, nl/s	Decrease, %
S group	250.6±7.5	249.4±4.5	
R1h	79.8±5.5	249.5±8.2*	68.0±3.0*
R1day	86.5±8.0	250.8±10.2*	65.5±2.0*
R7day	148.3±9.1	260.2±7.5*	43.0±2.5*
R14day	165.1±8.8	238.6±11.0*	30.8±3.4*
R28day	224.3±7.5	253.5±9.5*	11.5±2.0*

* $p < 0.01$ vs. SBF in the contralateral hemisphere.

MCAO and 1, 7, 14 and 28 Days of Reperfusion

After 1, 7 and 14 days of reperfusion, arterioles gradually increased in number and length; at 28 days of reperfusion, pial arteriolar networks regained diameter ratio as in the S group, but the length and branching ratios were higher and lower, respectively (table 1; fig. 2). Pial networks were characterized by arcading anastomotic arterioles overlapping the necrotic core. These vessels appeared at 7 days of reperfusion and were progressively longer; in the R28day group, there were the most vessels compared to all previous ischemic groups. Order 2 and order 1 anastomotic arterioles gave origin to order 2 and order 1 vessels, respectively (table 3).

Penetrating pial arterioles gradually increased in number in the R1day, R7day and R14day groups, surpassing S group values in the R28day group (table 3).

Microvascular permeability, marked in the R1day group, progressively decreased in the R7day, R14day and R28day groups (table 4). The same time-dependent changes were observed for leukocyte adhesion, progressively decreasing according to increasing reperfusion time. Conversely, PCD gradually increased, up to 28 days of reperfusion (85.0 ± 1.2 cm-1, $p < 0.01$ vs. S group) (table 4).

SBF, markedly reduced by 65.5 ± 2.0% in the R1day group ($p < 0.01$ vs. contralateral SBF 250.8 ± 10.2 nl/s), progressively increased up to 28 days of reperfusion, regaining 89.5 ± 2.2% of contralateral SBF (table 5).

Pial arterioles, unresponsive to topically applied Ach or Pap after 1 day of reperfusion, gradually recovered dilation, up to 28 days of reperfusion, not significantly different from the S group response (table 4).

Venular networks were characterized by a progressive increase in the number of perfused vessels from day 1 (where larger venules were perfused) up to 14 days of reperfusion (when the number of perfused vessels was in the same range as in contralateral pial microcirculation). At 28 days of reperfusion, venules were comparable in number with those observed in the S group.

The physiological parameters such as hematocrit, MABP, heart rate, pH, PCO_2 and PO_2 did not change in the different experimental groups.

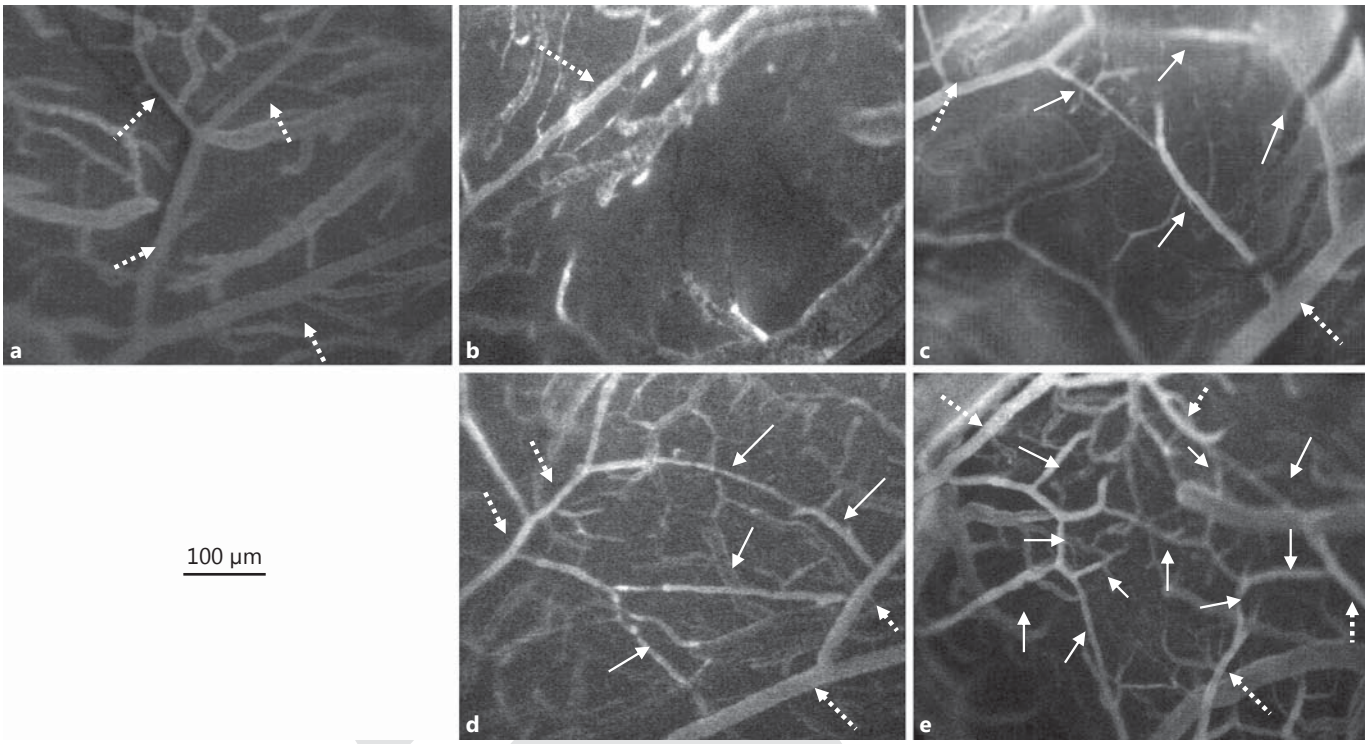

Fig. 2. Computer-assisted images of rat pial microvascular network: under baseline conditions (**a**), after 2-hour MCAO and 1-hour reperfusion (R1h group) (**b**), after 2-hour MCAO and 7-day reperfusion (R7day group) (**c**), after 2-hour MCAO and 14-day reperfusion (R14 day group) (**d**) and after 2-hour MCAO and 28-day reperfusion (R28day group) (**e**). Broken arrows represent penumbra preexistent arterioles and solid arrows represent anastomotic arterioles. Scale bar = 100 µm.

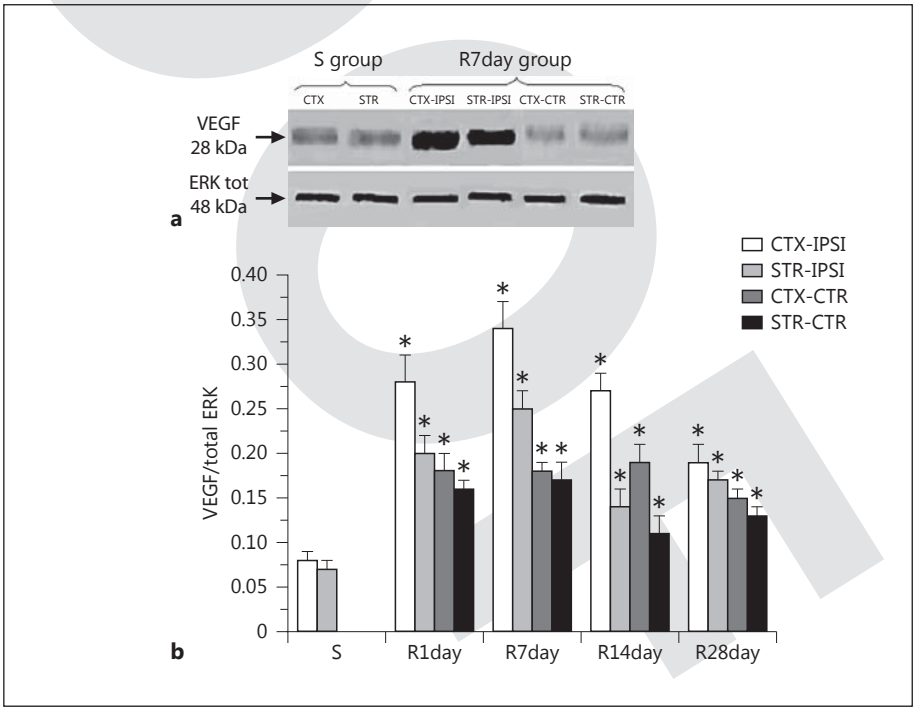

Fig. 3. a Western blotting of VEGF expression in the cortex and striatum of the affected hemisphere (CTX-IPSI and STR-IPSI) and of the contralateral hemisphere (CTX-CTR and STR-CTR) in the S group and in the R7day group. **b** The corresponding densitometric values (mean ± SEM) were expressed as arbitrary units and calculated for each experimental group and normalized on the basis of the respective ERK levels. Each experiment was repeated 3 times. * $p < 0.01$ vs. the S group.

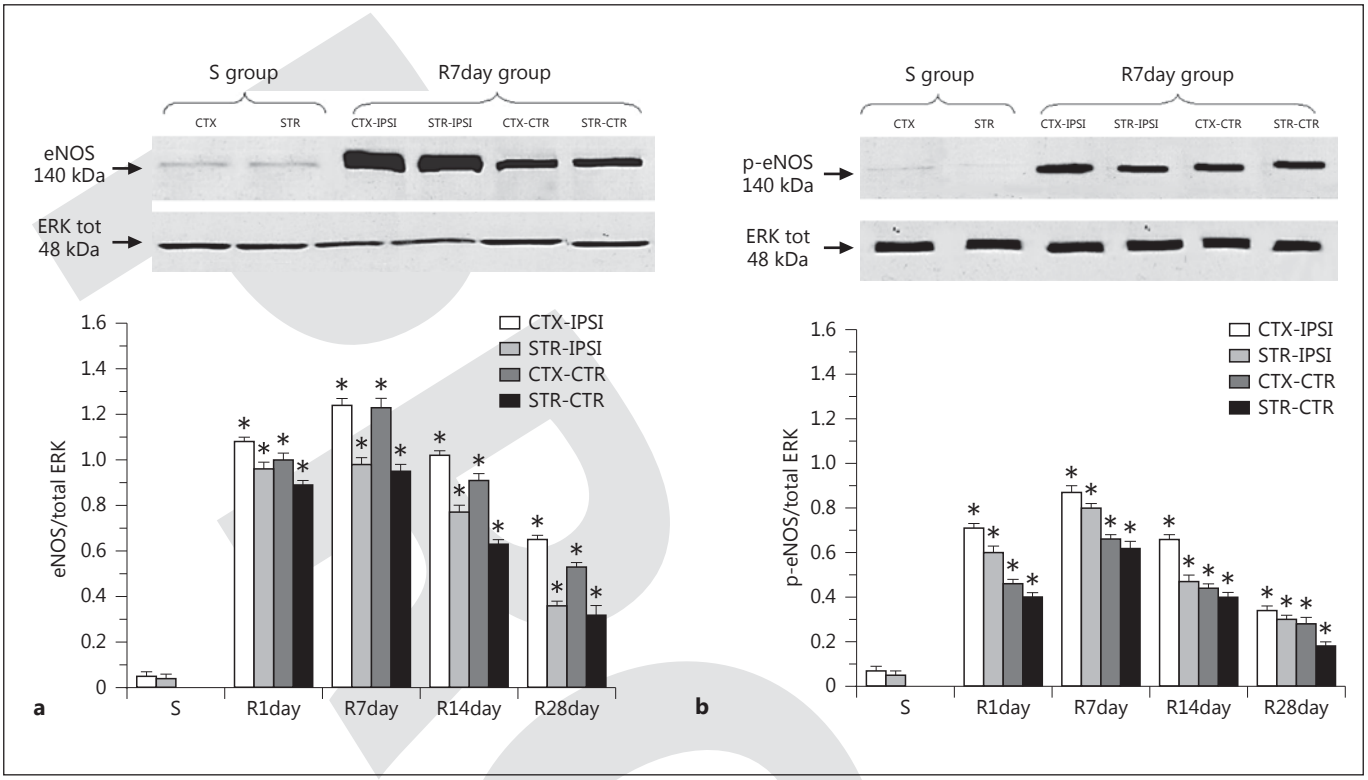

Fig. 4. Western blotting of eNOS (**a**) and phosphorylated eNOS (p-ENOS) (**b**) expression in the cortex and striatum of affected hemisphere (CTX-IPSI and STR-IPSI) and of contralateral hemisphere (CTX-CTR and STR-CTR) in the S group and in the R7day group; the corresponding densitometric values (mean ± SEM) were expressed as arbitrary units and calculated for each experimental group and normalized on the basis of the respective ERK levels. Each experiment was repeated 3 times. * $p < 0.01$ vs. the S group.

VEGF, eNOS, nNOS and iNOS Expression

VEGF expression increased significantly in the affected hemisphere compared to in the contralateral or sham-operated ipsilateral hemisphere. VEGF protein concentrations were higher in the cortex and striatum, peaking after 7 days of reperfusion, still increased at 14 days and decreased at 28 days (fig. 3).

eNOS protein concentrations significantly increased in the affected hemisphere compared to the contralateral or sham-operated ipsilateral hemisphere. Total eNOS protein expressions were higher in the cortex and striatum, peaking after 7 days of reperfusion, still increased at 14 days and reduced at 28 days of reperfusion (fig. 4). Phosphorylated eNOS proteins increased to a lesser extent than total eNOS ones in the cortex and striatum. The expression was higher in the affected hemisphere compared to the contralateral or sham-operated ipsilateral hemisphere (fig. 4).

In the R1day group, nNOS significantly increased in the ipsilateral cortex. The increase was higher in the ipsilateral striatum compared to the contralateral or sham-operated ipsilateral hemisphere at 7 days of reperfusion, decreasing severely afterwards (fig. 5). In the R1day and R7day groups, iNOS significantly increased in the ipsilateral cortex and striatum compared to the contralateral or sham-operated ipsilateral hemisphere. Thereafter, there was a marked decrease in expression (fig. 5).

Tissue Damage Evaluation

The R1h group showed marked lesions (an index of neuronal loss) in the cortex and striatum in the affected hemisphere (45.5 ± 3.5% of the ipsilateral hemisphere) compared to the S group (fig. 6). The cerebral lesions had increased progressively in size at day 1 of reperfusion (58.5 ± 3.1%), were pronounced at day 7 (48.9 ± 2.8%) and were decreasing by day 14 (41.3 ± 2.5%) and day 28 (18.2 ± 0.9%) (fig. 6).

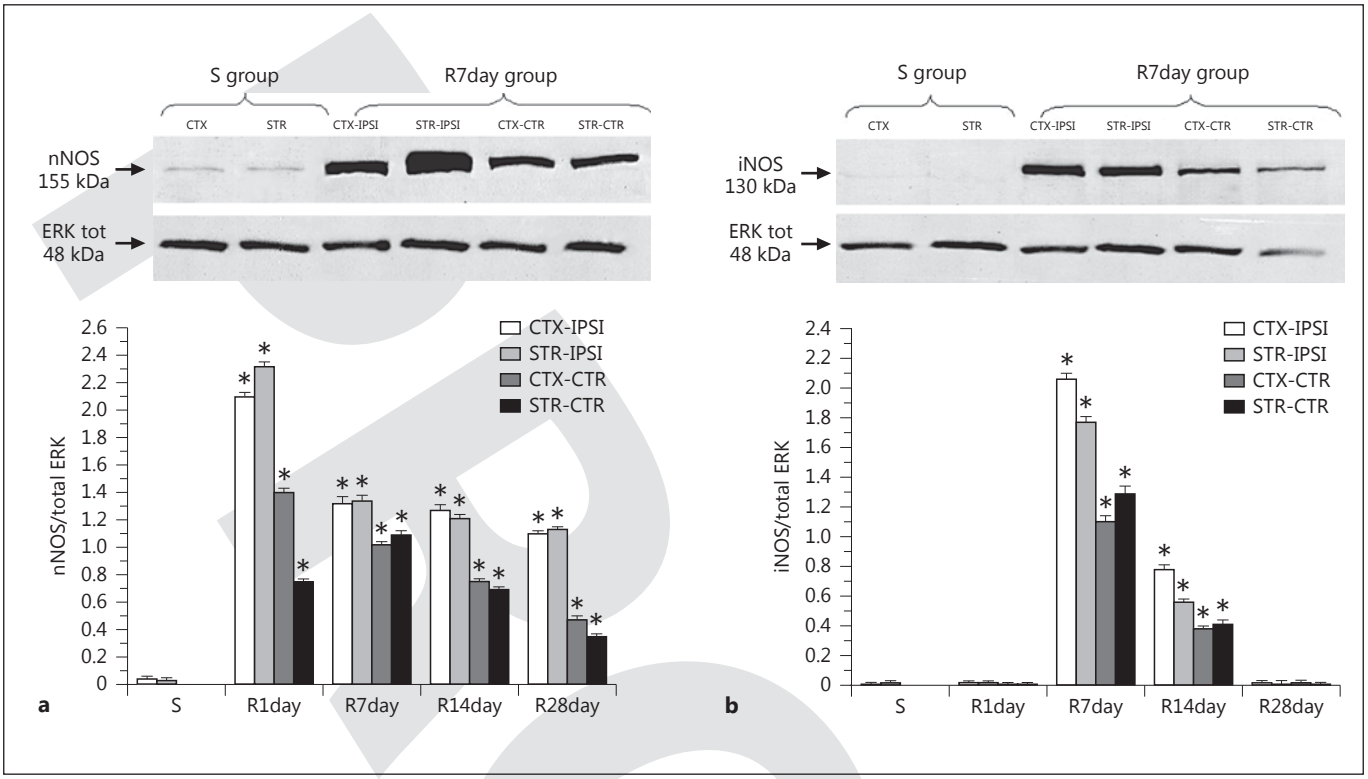

Fig. 5. Western blotting of nNOS (**a**) and iNOS (**b**) expression in the cortex and striatum of the affected hemisphere (CTX-IPSI and STR-IPSI) and of the contralateral hemisphere (CTX-CTR and STR-CTR) in the S group and in the R7day group; the corresponding densitometric values (mean ± SEM) were expressed as arbitrary units and calculated for each experimental group and normalized on the basis of the respective ERK levels. Each experiment was repeated 3 times. * $p < 0.01$ vs. the S group.

Neurological Assessment

No significant differences in the behavioral tests were detected among the experimental groups before MCAO; the score was 0 (normal). The R1day group presented severe motor and sensory abnormalities and was graded 11.0 ± 0.3 ($p < 0.01$ vs. baseline conditions). With longer reperfusion time, all animals showed a progressive decrease in behavioral deficits. TheR28day group recovered from neurological damage: the score was 2.0 ± 0.5 (mild injury; $p < 0.01$ vs. baseline conditions) (fig. 6).

Discussion

Our results indicate that the postischemic penumbra induced by MCAO is a site of intense microvascular reorganization, characterized by new vessel connections resulting in several anastomotic arterioles.

MCAO for 2 h and subsequent reperfusion for 1 h established an ischemic zone devoid of vessels, while the penumbra area presented a few arterioles, capillaries, larger venules and marked microvascular permeability as well as leukocyte adhesion. These results agree with the observations by del Zoppo [36], because immediate events include the breakdown of the primary endothelial cell barrier, plasma leakage and the expression of endothelial cell leukocyte adhesion receptors. However, we would like to note that greater permeability was triggered by mechanisms independent of leukocyte adhesion, even though leukocyte adhesion increased fluorescent dextran leakage.

After 7 and 14 days of reperfusion, perfused arterioles progressively increased in number, showing a different geometric arrangement. Parent vessels were connected to smaller arterioles than in the S group, characterized by order $n + 1$ arterioles giving origin to most order n vessels as shown by the connectivity matrix. In ischemic animals

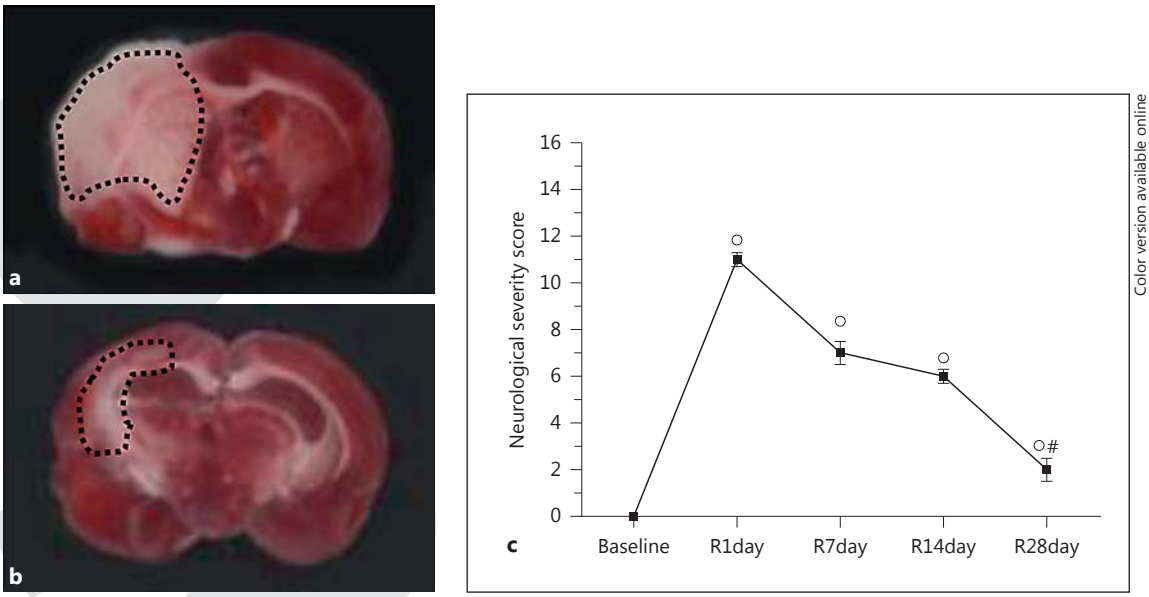

Fig. 6. TTC staining of a coronal brain slice from a rat submitted to MCAO and 1 day of reperfusion. **a** The lesion in the cortex and striatum is outlined by the dashed black line. **b** TTC staining of a coronal brain slice from a rat submitted to MCAO and 28 days of reperfusion, where injury was reduced. **c** Neurological severity scores in the different experimental groups. R1day group: 2-hour MCAO and 1-day reperfusion, R7day group: 2-hour MCAO and 7-day reperfusion, R14day group: 2-hour MCAO and 14-day reperfusion, R28day group: 2-hour MCAO and 28-day reperfusion compared with baseline conditions for each rat prior to MCAO (0 score, baseline). * $p < 0.01$ vs. baseline; † $p < 0.01$ vs. the other experimental groups.

Table 6. Infarct size of the striatum and cortex expressed as percentage of the whole ipsilateral cerebral hemisphere in each experimental group

Group	Striatum	Cortex
S group	0	0
R1h	72.3±1.8*	68.5±2.3*
R1day	71.5±1.5*	65.1±2.7*
R7day	57.0±2.2 *	60.3±3.1*
R14day	42.5±3.0*	48.7±2.1*
R28day	20.8±2.7*, **	31.5±2.0*, **

* $p < 0.01$ vs. S group; ** $p < 0.01$ vs. other experimental groups.

at days 7 and 14 of reperfusion, parent vessels were not connected with (a majority of) daughter vessels of an immediately successive order; therefore, an order gap was observed, i.e. predominant connections of the largest with the smallest arterioles, which was completely different from the S group.

It is reasonable to suggest that the increase in the number of perfused arterioles at day 1 of reperfusion might have been due to reperfusion or reopening of preexistent arterioles. At day 7 of reperfusion, new branchings were likely due to new vessel formation and connections, as suggested by anastomotic arterioles appearing after 7 days and increasing in number at day 14 of reperfusion. These vessels constituted arteriolar arcades overlapping and supplying blood to the ischemic core. Vascular remodeling was complex and involved vessel adjustment in length and branchings until day 28 of reperfusion.

Penetrating vessels, i.e. pial arterioles supplying the outer cortical layers, disappeared after MCAO and reappeared after 7 days of reperfusion, increasing in number at day 14 and surmounting the S group-operated animal values at day 28 of reperfusion. According to different time points during reperfusion, the PCD increased with the same temporal pattern as was observed with penetrating arterioles.

Microvascular leakage, marked after R1h, time-dependently diminished over time, as did leukocyte adhesion. Arteriolar responsiveness to Ach and Pap, compromised after MCAO, recovered progressively, starting at day 7 of reperfusion.

Up to day 14 of reperfusion, the number of perfused venous vessels in the penumbra area increased progres-

sively, while SBF recovered progressively for up to 28 days. Therefore, it is reasonable to suggest that venular network remodeling mostly involved the reopening and reperfusion of preexisting venules, due to a low or moderate increase in the number of new vessels, whereas arterioles appeared more affected by remodeling, as indicated by an increase in anastomotic vessels. During reperfusion, contralateral pial microcirculation in rats submitted to MCAO did not present any geometric or functional changes compared to the S group, as previously reported [36, 37]. The poststroke neovascularization phenomenon has long been debated and is still questioned. Mostany et al. [6] noted that at 90 days of reperfusion after MCAO, mouse cerebral microvasculature does not undergo angiogenesis because the branching nodes do not increase. It is important to note that these observations were carried out 1.3 mm from the infarct edge. Therefore, in mouse cerebrovasculature, no angiogenesis outside the infarct zone after MCAO excludes rearrangement of microvessels within 90 days of injury.

Conversely, several studies on mice or rats submitted to transient or permanent MCAO indicate the proliferation of endothelial cells in the penumbra as early as 12–24 h following vessel damage, with an increased number of vessels afterwards [8, 9]. Active angiogenesis takes place 3–4 days after ischemic insult in humans [10]. Hayashi et al. [8] reported long-lasting vessel proliferation for more than 21 days after brain ischemia. Tomita et al. [11] observed new vessel formation in a mouse chronical cranial window preparation 30 days after permanent ischemia, even though they did not differentiate the vessel orders. Beck and Plate [18], Garcia et al. [38] and Zhang et al. [39] reported several evidences suggesting neovascularization occurs after focal cerebral ischemia. Our data indicate that the pial microvasculature may undergo complex remodeling: the vessels of new origin developed into smaller vessels and extended into the ischemic core by sprouting or intussusception 2–28 days after the onset of cerebral ischemia. Remodeling was characterized by new arterioles overlapping the ischemic core.

Concurrent with this was the increase in expression of VEGF at day 1 of reperfusion, peaking at day 7. Our data support previous observations indicating that VEGF expression increases in the rodent brain during ischemia-reperfusion, peaking at 7 days within the penumbra area: upregulated VEGF is colocalized with neovascularization [40–42].

Our results indicate an increase in the expression of NOS isoforms (e-NOS, n-NOS and i-NOS): eNOS expression in the cortex and striatum of the affected hemisphere increased significantly when compared to the ipsilateral cortex and striatum of the S group animals at day 1, peaking at day 7, being highest at day 14 and decreasing at day 28 of reperfusion. Therefore, pial arteriolar remodeling appears to be accompanied by increased eNOS expression.

nNOS expression markedly increased at days 1 and 7 of reperfusion, indicating a pronounced neuronal damage in the first days after ischemia, as previously suggested [14, 15].

Previous experiments in mutant mice subjected to models of focal ischemia demonstrate that nNOS mutant animals develop smaller infarcts, consistent with a role for nNOS in neurotoxicity following cerebral ischemia [43]. In our model, nNOS expression increased in the first days after ischemia, coincident with higher brain damage, indicated by marked microvascular changes, TTC staining of brain slices and behavioral tests. The neuronal recovery, proved by behavioral tests, was paralleled by a decrease in nNOS expression accompanied by intense vascular remodeling.

The increase in iNOS expression at days 1 and 7, thereafter markedly decreasing up to day 28 of reperfusion, may indicate the activation of an inflammatory response by ischemia. Previous data indicate that inhibition of iNOS expression by aminoguanidine is able to reduce infarct size in brain ischemic injury; therefore, the increase in iNOS appears to contribute to tissue inflammation triggered by ischemia, characterized by marked microvascular permeability and leukocyte adhesion in our model [44].

Generally, all NOS isoforms were activated with different time-dependent involvement, likely indicating a complex interaction between VEGF and NOS isoform expressions. VEGF has been suggested as a common trigger of all NOS isoform activation [18]; our data demonstrate that time-dependent expressions of VEGF and eNOS strictly corresponded. For nNOS and iNOS expression, we cannot exclude VEGF involvement, but early activation and faster inactivation of both these isoforms may suggest a marked influence of neuronal damage and an inflammatory response, respectively.

Vascular remodeling was paralleled by the amelioration of neuronal damage, as indicated by TTC staining of brain slices up to day 28 of reperfusion. This was accompanied by behavioral data from the battery of functional tests demonstrating that motor and sensory functions progressively recovered after ischemic insult. Significantly better performances were detected at day 28 of reperfusion than at other time points during reperfusion. Therefore, neuronal recovery accompanied vascular remodeling.

In conclusion, pial vascular remodeling after transient MCAO mainly involves arteriolar networks. An increasing number of anastomotic arcading arterioles characterize pial microvasculature. These arcades are likely vessels sprouting from preexistent arterioles localized in the penumbra area, able to overlap the ischemic core. Remodeling mechanisms appeared to be accompanied by a higher expression of VEGF and eNOS likely modulating angiogenesis in vivo. Finally, cerebral microvessel remodeling was accompanied by improved neurological behavior.

Appendix

Matrix Description of Branching Pattern

In general, vessels of order *n* may spring from vessels of orders $n + 1$, $n + 2$, … as established by the diameter-defined Strahler model. In this scheme, each blood vessel between 2 nodes of bifurcation is called a segment. Segments connected in series function as a single tube in hemodynamics; each tube is called an element.

A more realistic mathematical model of the pial vasculature can be presented in the form of a matrix, the component of which in row *n* and column *m* is the ratio of the total number of elements of order *n*, sprung from elements of order *m*, divided by the total number of elements in order *m*. To experimentally obtain the matrix, we must group all the vascular branches into elements, then record for each element of order *m* the number of element of orders *m*, *m*-1, *m*-2,… that arise directly from that element. Statistics were then used to obtain the mean values and SEM of each component of the matrix.

Table 2a reports the connectivity matrix for the S group. Column 4 of order *m*, the last one on the right, represents the ratio of order 1, order 2 and order 3 vessel number divided by the total number of order 4 arterioles. Ten arterioles have been classified and studied as order 4 vessels. The number of order 1 arterioles, coming from the parent order 4, can be obtained by multiplying 0.49 by 10; in total, five order 1 arterioles originate from order 4 parent vessels. The number of order 2 arterioles originating from the same order 4 parent is obtained by multiplying 1.43 by 10; therefore, fourteen order 2 arterioles have originated from order 4 parent vessels. The number of order 3 arterioles is calculated by multiplying 2.50 by 10; in total, there are twenty-five order 3 arterioles coming from order 4 parent vessels. The number of order 4 arterioles, originating from the same order 4 parent vessels, can be obtained by multiplying 0.15 by 10; in total, there is only one order 4 arteriole.

From column 3 of order *m*, the number of order 3, 2 and 1 vessels coming from parent order 3 arterioles can be obtained as described above. Calculation has also been carried out in the other columns.

Therefore, in the S group animals, order 4 arterioles gave origin to most order 3 vessels, several order 2 arterioles and few order 1 vessels. No vessels of order 0 (capillaries) originated from order 4 arterioles. Order 3 arterioles were connected to most order 2 vessels, few order 1 arterioles and no capillaries, while order 2 and order 1 vessels gave origin to most order 1 arterioles and capillaries, respectively.

In the R1day, R7day and R14day groups, a connectivity matrix demonstrates that order 4 arterioles gave rise to most order 2 vessels and few order 3 and 1 arterioles (table 2b–d); in the R28day group, order 4 arterioles gave rise to most order 3 vessels, few order 2 vessels and no order 1 vessels or capillaries (table 2e).

References

1 Gibbons GH, Dzau VJ: The emerging concept of vascular remodeling. N Engl J Med 1994; 330:1431–1438.
2 Wagner S, Tagaya M, Koziol JA, Quaranta V, del Zoppo GJ: Rapid disruption of an astrocyte interaction with the extracellular matrix mediated by integrin $\alpha_6\beta_4$ during focal cerebral ischemia/reperfusion. Stroke 1997;28: 858–865.
3 Cipolla MJ, Lessov N, Hammer ES, Curry AB: Threshold duration of ischemia for myogenic tone in middle cerebral arteries: effect on vascular smooth muscle actin. Stroke 2001;32: 1658–1664.
4 Ames A, Wringht LW, Kowade M, Thurston JM, Majno G: Cerebral ischemia: II. The no-reflow phenomenon. Am J Pathol 1968;52: 437–453.
5 Kuroda S, Siesjö BK: Reperfusion damage following focal ischemia: pathophysiology and therapeutic windows. Clin Neurosci 1997;4: 199–212.
6 Mostany R, Chowdhury TG, Johnston DG, Portonovo SA, Carmichael ST, Portera-Cailliau C: Local hemodynamics dictate long-term dendritic plasticity in peri-infarct cortex. J Neurosci 2010;30:14116–14126.
7 Leventhal C, Rafii S, Rafii D, Shahar A, Goldman SA: Endothelial trophic support of neuronal production and recruitment from the adult mammalian subependymal. Mol Cell Neurosci 1999;13:450–464.
8 Hayashi T, Noshita N, Sugawara T, Chan PH: Temporal profile of angiogenesis and expression of related genes in the brain after ischemia. J Cereb Blood Flow Metab 2003;23: 166–180.
9 Marti HJ, Bernaudin M, Bellail A, Schoch H, Euler M, Petit E, Risau W: Hypoxia-induced vascular endothelial growth factor expression precedes neovascularization after cerebral ischemia. Am J Pathol 2000;156:965–976.
10 Krupinski J, Kaluza J, Kumar P, Kumar S, Wang JM: Role of angiogenesis in patients with cerebral ischemia stroke. Stroke 1994;25: 1794–1798.
11 Tomita Y, Pinard E, Tran-Dinh A, Schiszler I, Kubis N, Tomita M, Suzuki N, Seylaz J: Long-term, repeated measurements of mouse cortical microflow at the same region of interest with high spatial resolution. Brain Res 2011; 1372:59–69.
12 Zhang F, White JG, Iadecola C: Nitric oxide donors increase blood flow and reduce brain damage in focal ischemia: evidence that nitric oxide is beneficial in the early stages of cerebral ischemia. J Cereb Blood Flow Metab 1994;14:217–226.
13 Iadecola C, Zhang F, Xu S, Casey R, Ross ME: Inducible nitric oxide synthase gene expression in brain following cerebral ischemia. J Cereb Blood Flow Metab 1995;15:378–384.
14 Wei G, Dawson VL, Zweier JL: Role of neuronal and endothelial nitric oxide synthase in nitric oxide generation in the brain following cerebral ischemia. Biochim Biophys Acta 1999;1455:23–34.
15 Moro MA, Càrdenas A, Hurtado O, Leza JC, Lizasoain I: Role of nitric oxide after brain ischemia. Cell Calcium 2004;36:265–275.

16 Hayashi T, Abe K, Suzuki H, Itoyama Y: Rapid induction of vascular endothelial growth factor gene expression after transient middle cerebral artery occlusion in rats. Stroke 1997; 28:2039–2044.
17 Plate KH, Beck H, Danner S, Allegrini PR, Wiessner C: Cell type specific upregulation of vascular endothelial growth factor in an MCA-occlusion model of cerebral infarct. J Neuropathol Exp Neurol 1999;58:654–666.
18 Beck H, Plate KH: Angiogenesis after cerebral ischemia. Acta Neurophatol 2009;117:481–496.
19 Lapi D, Marchiafava PL, Colantuoni A: Pial microvascular responses to transient bilateral common carotid artery occlusion: effects of hypertonic glycerol. J Vasc Res 2008;45:69–77.
20 Hudetz AG, Oliver JA, Wood JD, Newman PJ, Kampine JP: Leukocyte adhesion in pial cerebral venules after PMA stimulation and ischemia/reperfusion in vivo. Adv Exp Med Biol 1997;411:513–518.
21 Kroll J, Waltenberger J: VEGF-A induces expression of eNOS and iNOS in endothelial cells via VEGF receptor-2 (KDR). Biochem Biophys Res Commun 1998;252:743–746.
22 Yamashita T, Ninomiya M, Hernandez AP, Garcia-Verdugo JM, Sunabori T, Sakaguchi M, Adachi K, Kojima T, Hirota Y Kawase T, Araki N, Abe K, Okano H, Sawamoto K: Subventricular zone-derived neuroblasts migrate and differentiate into mature neurons in the post-stroke adult striatum. J Neurosci 2006; 26:6627–6636.
23 Chen J, Li Y, Wang L, Lu M, Zhang X, Chopp M: Therapeutic benefit of intravenous administration of bone marrow stromal cells after cerebral ischemia in rats. Stroke 2001;32: 1005–1011.
24 Mayhan WG, Patel KP: Treatment with dimethylthiourea prevents impaired dilatation of the basilar artery during diabetes mellitus. Am J Physiol 1998;274:H1895–H1901.
25 Osol G, Laher I, Cipolla M: Protein kinase C modulates basal myogenic tone in resistance arteries from the cerebral circulation. Circulation Res 1991;68:359–367.
26 Longa EZ, Weinstein PR, Carlson S, Cummins R: Reversible middle cerebral artery occlusion without craniectomy in rats. Stroke 1989;20:84–91.
27 Garcia JH, Yoshida Y, Chen H, Li Y, Zhang ZG, Lian J, Chen S, Chopp M: Progression from ischemic injury to infarct following middle cerebral artery occlusion in the rat. Am J Pathol 1993;142:623–635.
28 del Zoppo GJ, Sharp FR, Heiss WD, Albers GW: Heterogeneity in the penumbra. J Cereb Blood Flow Metab 2011;31:1836–1851.
29 Ngai AC, Ko KR, Morii S, Winn HR: Effect of sciatic nerve stimulation on pial arterioles in rats. Am J Physiol 1988;254:H133–H139.
30 Golanov EV, Yamamoto S, Reis DJ: Spontaneous waves of cerebral blood flow associated with a pattern of electrocortical activity. Am J Physiol 1994;266:R204–R214.
31 Kassab GS, Lin DH, Fung YC: Morphometry of pig coronary arterial trees. Am J Physiol 1993;256:H350–H365.
32 Lapi D, Marchiafava PL, Colantuoni A: Geometric characteristics of arterial network of rat pial microcirculation. J Vasc Res 2008;45: 69–77.
33 Shih AY, Friedman B, Drew PJ, Tsai PS, Lyden PD, Kleinfeld D: Active dilation of penetrating arterioles restores red blood cell flux to penumbral neocortex after focal stroke. J Cereb Blood Flow Metab 2009;29:738–751.
34 Matrone C, Pignataro G, Molinaro P, Irace C, Scorziello A, Di Renzo GF, Annunziato L: HIF-1alpha reveals a binding activity to the promoter of iNOS gene after permanent middle cerebral artery occlusion. J Neurochem 2004;90:368–378.
35 Bederson JB, Pitts LH, Germano SM, Nishimura MC, Davis RL, Bartkowski HM: Evaluation of 2,3,5-triphenyltetrazolium chloride as a stain for detection and quantification of experimental cerebral infarction in rats. Stroke 1986;17:1304–1308.
36 del Zoppo GJ: Stroke and neurovascular protection. N Engl J Med 2006;354:553–555.
37 Chen J, Zacharek A, Zhang C, Jiang H, Li Y, Roberts C, Lu M, Kapke A, Chopp M: Endothelial nitric oxide synthase regulates brain-derived neurotrophic factor expression and neurogenesis after stroke in mice. J Neurosci 2005;25:2366–2375.
38 Garcia J, Cox J, Uudgins W: Ultrastructure of the microvasculature in experimental cerebral infarction. Acta Neuropathol 1971;18: 273–285.
39 Zhang ZG, Zhang L, Jiamg Q, Zhang R, Davies K, Powers C, Bruggen N, Chopp M: VEGF enhances angiogenesis and promotes blood-brain barrier leakage in the ischemic brain. J Clin Invest 2000;106:829–838.
40 Pettersson A, Nagy JA, Brown LF, Sundberg C, Morgan E, Jungles S, Carter R, Krieger JE, Manseau EJ, Harvey VS, Eckelhoefer IA, Feng D, Dvorak AM, Mulligan RC, Dvorak HF: Heterogeneity of the angiogenic response induced in different normal adult tissues by vascular permeability factor/vascular endothelial growth factor. Lab Invest 2000;80:99–115.
41 Croll SD, Weigand SJ: Vascular growth factors in cerebral ischemia. Mol Neurobiol 1999;155:1915–1927.
42 Plate KH: Mechanisms of angiogenesis in the brain. J Neuropathol Exp Neurol 1999;58: 313–320.
43 Huang PL: Neuronal and endothelial nitric oxide synthase gene knockout mice. Braz J Med Biol Res 1999;32:1353–1359.
44 Danielisova V, Burda J, Nemethova M, Gottlieb M: Aminoguanidine administration ameliorates hippocampal damage after middle cerebral artery occlusion in rat. Neurochem Res 2011;36:476–486.